LOAD FREQUENCY CONTROL SCHEME FOR A MICROGRID SYSTEM WITH THE APPLICATION OF hTLO-DE ALGORITHM

Indrajit Koley[1,*] - Asim Datta[2] - Goutam Kumar Panda[3]

[1]Department of Electrical Engineering, Siliguri Institute of Technology, Siliguri-734009, India
[2]Department of Electrical Engineering, Tezpur University, Tezpur, Assam-784028, India
[3]Department of Electrical Engineering, Jalpaiguri Government Engineering College, Jalpaiguri-735102, India

ARTICLE INFO

***Article history*:**
Received: 23.12.2021.
Received in revised form: 02.05.2022.
Accepted: 10.05.2022.

Keywords:
Load frequency control (LFC)
Diesel/wind/battery
Microgrid system
hTLO-DE algorithm
PIDD controller

DOI: https://doi.org/10.30765/er.1925

Abstract:

Load frequency control (LFC) is a crucial feature of electric power systems to maintain a balance between power supply and load demand, thus avoiding a deviation of the grid frequency. The present work aims to implement an effective LFC scheme for a microgrid system consisting of a diesel generator (DEG), a wind turbine generator (WTG) and a battery storage system. Proportional-integral-double-derivative (PIDD) controllers are used to implement the proposed LFC scheme. The controller parameters are computed using an innovative hybrid teaching-learning-optimization differential-evaluation (hTLO-DE) algorithm. The main scope of the work lies in application of hTLO-DE optimized PIDD controllers in DEG-WTG-battery storage based MG system. The results obtained with PIDD controllers are compared with those obtained with the traditional PI and PID controllers. A critical analysis shows that the PIDD controller can provide better dynamic responses in terms of settling time and magnitude of oscillations compared to PI and PID controllers. The frequency responses of the system are studied under different scenarios of generation and load variations, which establishes the robustness of the proposed PIDD-based LFC scheme.

1 Introduction

Microgrid is defined as the arrangement of a local electric power network using regulated loads and distributed energy resources (DERs) like wind turbine generators (WTG), diesel generators (DEG), battery storage, and so on [1]. Considering the current fossil fuel crisis and environmental problems, renewable energy sources (RESs) are gaining importance. Conversely, the conventional fossil fuel based generation is always reliable as does not depend on weather conditions. The idea of mixing renewable and conventional energy generations relies on the equilibrium among the reliability in generation, cost of generation, and environmental issues [2]. But in connection with the renewable energy-based distributed generations (DGs), there are many challenges like controllability, islanding operation, stability of the system, etc. [3]. The grid controls the voltage and frequency at the DG interconnection points in grid-connected mode. Nonetheless, the fundamental problem in operating a renewable energy-based DG in islanded mode is its stability. In non-islanded mode, the power storage system in a microgrid can support the power balance [4], but a competent LFC method is needed to maintain the system frequency [5].

The goal of LFC is to minimize the frequency deviation by regulating the power flow of DERs in the system. Therefore, system frequency and tie-line power flows are monitored and generation within the region is adjusted to keep the time average of the area control error (ACE) constant. In LFC, ACE is commonly used as a measure of regulation. To achieve a lower ACE, both the tie-line power and frequency errors should be

[*] *Corresponding author*
E-mail address: indrajit.koley@gmail.com

close to zero. Due to the high percentage of irregular renewable energy, fluctuations in power generation cause frequent imbalance between supply and demand [6], which leads to frequency deviations in the microgrid. Frequency stability is very critical for AC systems. Researchers have proposed a number of solutions to achieve LFC in power systems in recent decades, namely adaptive control [7], intelligent control [8], robust control [9], model predictive control (MPC) [10], etc. Although conventional PI or PID controllers have been used in LFC applications, they show their limitations in RES based systems [11]. The distributed control technique was first introduced in [12]. Lately, a number of methods were proposed in this field [20]. In these works, agents are adjusted using local controllers by sensing local signals. Thus, in distributed control has the highest degree of freedom [13]. Moreover, it is seen that distributed strategies are more suitable for handling a multiple number of low-capacity DGs [14]. However, these approaches still have some drawback due to non-optimum responses and a high probability for instability [15].

In recent decades, researchers have been using several optimization procedures to deal with the computation of control parameters. The main difficulty in LFC is the designing controllers with optimal gain parameters. Researchers have suggested a variety of optimization strategies, including the firefly algorithm (FA) [16], bacterial foraging (BFO) optimization [17], fruit fly algorithm (FFA) [18], cuckoo search algorithm (CSA) [19], and artificial bees' colony (ABC) algorithm [20], to find-out the optimal parameters for load frequency controllers. Recently, hybrid optimization algorithms have attracted the research communities due to usefulness in finding global optimal values under multi-uncertainties [21]. Panwar et al. [22] have applied hybrid improved BFO-PSO technique in tuning controllers for LFC applications.

From the literatures it can be observed that several classical controllers were used [23]. Ali and Abd Elazim [17] used the BFOA technique to improve the parameters of the PID controller for the LFC problem and compared it to Ziegler Nichols (ZN) and GA optimization strategies. In the AGC problem, Sahu et al. [24] used a hybrid firefly method with a pattern search technique to create a PID controller. Parmar et al. [25] proposed a multi-source realistic model with an optimal output feedback controller based on output state variables. In a multi-area system, Sahu et al. [26] used TLBO with a Fuzzy PID controller. Sahu et al. [27] employed TLBO to tune IDD and PIDD controllers for a 2-area thermal system and extended to a varied source system. For enhancing responses in a multi-area system, Dash et al. [28],[29] presented a cascaded PD-PID controller adjusted by the BAT algorithm The use of a Kalman filter to construct a self-tuning optimizer for voltage flicker and harmonic estimates has been proposed by Panigrahi et al. [30]. For a multi-area system with automatic generation control, Barisal et al. [31] demonstrated hybrid PSO-LEVY flight algorithm tuned fuzzy-PID controllers. From the literature review, it is clear that, the use of tuning technique in finding optimal controller constraints, has a significant impact on the system functioning.

This paper presents application of a hybrid teaching-learning-optimization differential-evaluation (hTLO-DE) algorithm for computing design parameters of load frequency controllers in a DEG-wind-battery based microgrid system. Methodology wise, firstly, a system model with multiple DGs (DEG, WTG, battery storage) is developed; secondly, PIDD controllers are adopted for implementation of a LFC scheme; and thirdly, hTLO-DE computational technique is applied to optimize the design parameters. The main contributions of this work can be summarized as follows:

(a) A DEG-WTG-battery based microgrid system is modeled.
(b) PIDD controllers are adopted for LFC in the DEG-WTG-battery based microgrid system
(c) A hybrid hTLO-DE computational technique is applied to tune controlled parameters effectively.
(d) The PIDD controller responses are compared to those of the PI and PID controllers.
(e) The suggested controller and optimization approach is tested with load variation ranging from ±20% in the DEG area.

2 System Description and Modelling

The investigated microgrid system consists of DEG, WTG and battery system, as shown in Figure 1. Combined with the weather-dependent WTG and energy storage system, DEG is considered as a reliable source of active power. In the system modelling, PIDD controller and system parameters such as frequency bias parameter (B_i), governor speed regulation (R_i), and ACE_i are represented. The governor output signal, governor time constant, the time constant of the turbine, the change of the output power of the turbine, the gain

of the power system, the time constant of the system, the load changes, the synchronisation coefficient, incremental tie line power changes, and the frequency deviation are the other system considerations.

2.1. Diesel Generator (DEG)

The DEG is commonly employed as a stable source of electricity in microgrid schemes. It is necessary to alter the output of the DEG as the load demand varies. Figure 2 depicts the DEG transfer fiction (TF) model. In a first-order system, this model usually consists of a generator and a governor. Accordingly, t_{g1} refers to time constant (TC) for inertia delay, t_{t1} is TC for governor unit, t_1 is the TC for diesel generator, t_{p1} indicates TC of power system, and R_1 is the coefficient of speed regulation of DEG.

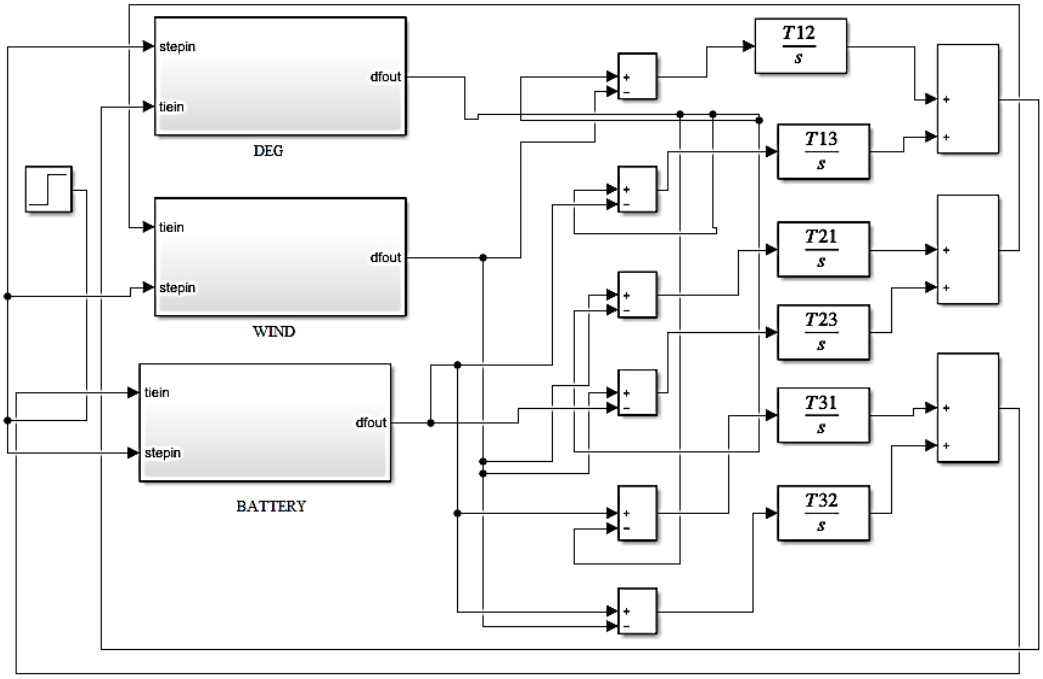

Figure 1. Investigated microgrid model.

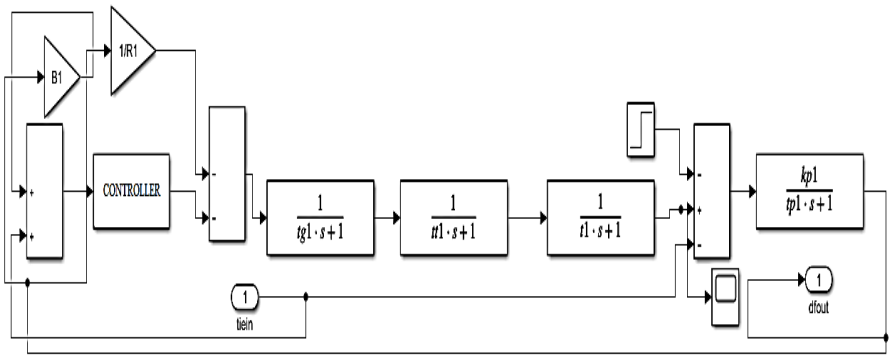

Figure 2. TF based representation of DEG system.

The TF representation of different components of the DEG system as represented in Figure 2 are as follow:

$\frac{1}{t_{g1}.s+1}$ = inertia delay unit, (1)

$\frac{1}{t_{t1}.s+1}$ = speed governing unit, (2)

$\frac{1}{t_1.s+1}$ = generator unit, (3)

$\frac{k_{p1}}{t_{p1}.s+1}$ = power system unit. (4)

2.1.1. Wind Turbine Generator (WTG)

WTG power output can be determined by wind speed (V_w), blade radius (r), pitch angle (β), air density (ρ), and power coefficient (C_P). The power output of a wind turbine can be expressed as follows:

$$P_m = \frac{1}{2}\pi\rho C_p(\lambda,\beta)R^2V_w^3, \quad (5)$$

$$\lambda = \frac{\omega R}{V_w}, \quad (6)$$

where λ = speed ratio and ω = speed of wind.
Figure 3. represents the TF model of WTG area.

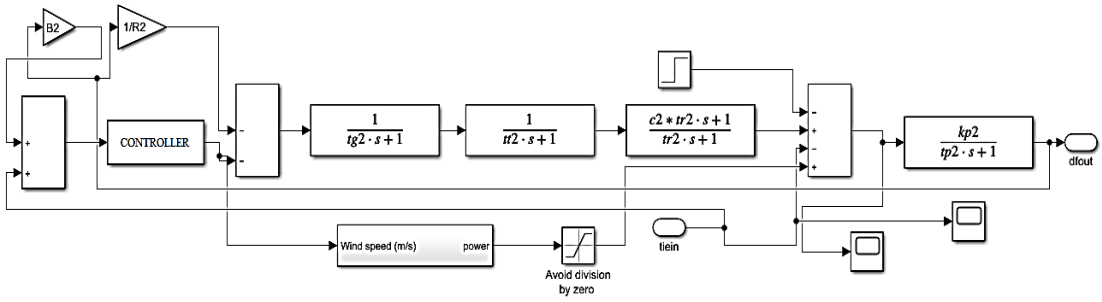

Figure 3. TF based representation of WTG system.

The power coefficient of wind turbine unit can be represented as:

$$C_P(\beta) = (0.44 - 0.0167\beta)\, sin\frac{(\pi(\lambda-2))}{15-0.3\beta} - 0.00184(\lambda-3)\beta. \quad (7)$$

At zero blade angle the optimal value of the tip speed ratio (λ_{opt}) for wind turbine blade is obtained and the wind power extracted from wind turbine can be written as:

$$P_w = K_{opt}V_w^3, \quad (8)$$

where K_{opt} is a constant defined as:

$$K_{opt} = 0.44\, sin\left(\frac{\pi(\lambda_{opt}-3)}{15}\right). \quad (9)$$

The different components of the wind energy system are represented with transfer function in Figure 3 as [32]:

$$\frac{1}{1+st_{t2}} = \text{wind turbine.} \quad (10)$$

Hydraulic pitch actuator controls the pitch angle of the turbine. The pitch angle is very finely selected to maximise the output power of WTG. The transfer function block for hydraulic pitch actuator may be given by (11):

$$\frac{1}{1+st_{g2}} = \text{pitch actuator system.} \quad (11)$$

The 'data fit pitch response' block of Figure 3 acts as a simple lag compensator which is required to match the phase/gain characteristic of the model:

$$\frac{c_2\, t_{r2}\, s+1}{t_{r2}\, s+1} = \text{data fit system,} \quad (12)$$

where t_{t2} is the TC for wind turbine, t_{g2} is the TC for pitch actuator system, t_{r2} is the TC for data fit system. Step load is applied to the system to find out the deviation of frequency of the system. The variation of wind speed is considered and controller takes care of the effect of that. The avoided division by zero block is applied so that infinite speed of the wind cannot be reached.

2.1.2 Battery System

Figure 4 depicts an aggregate model of a battery system. The battery charger's job is to regulate the power flow in between the grid and energy storage. R_{AG}, the coefficient of droop characteristics is considered as 2.4 Hz/pu. The TF representation of battery system and DC/AC converter units are as [24]:

$$\frac{1}{T_{EV}s+1} = \text{battery system,} \quad (13)$$

$$\frac{1}{T_{CON}s+1} = \text{DC/AC converter unit,} \quad (14)$$

where T_{EV} is the TC of the battery system. K_{EV} is reliant on the state-of-charge (SOC) of the battery. The advantage of P_{EV} is that it can be considered as a source of generating power during peak load hour and can also be considered as load during lightly loaded time and can become a contributor in LFC scheme. The P_{EV} can also be considered as ballistic load for power generation from renewable energy souses. T_{CON} is the TC for DC/AC converter circuit.

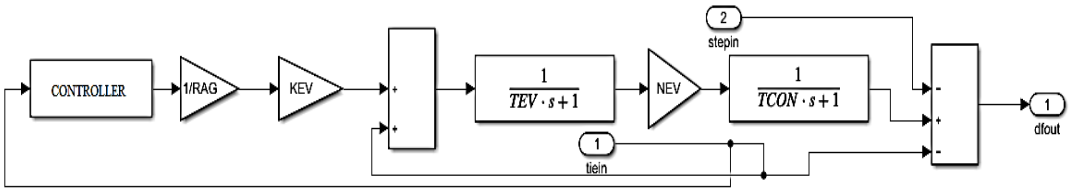

Figure 4. TF based model of battery system.

The choice of the objective function is critical for the controllers' optimal operation. Various objective functions have been employed by different researchers, including integral of time multiplied by absolute error (ITAE), integral of absolute error (IAE), integral of time multiplied by square error (ITSE), and integral of

square error (ISE). As a more sensitive criterion than IAE or ISE, the ITAE criterion efficiently regulates the settling time. An ITSE tuned controller, on the other hand, can provide a huge control signal, which can be problematic in the event of a sudden imbalance. The ITAE as represented in (15), is the cost function (*J*), which must be minimised for optimization. As a result, each area control error, A_{error}, is used to frame the goal function.

Thus, optimization function for the minimization of *J is* given as [33]:

$$J = ITAE = \int_0^{t_{sim}} t_{sim}\left[\sum_{i=1}^{N_{area}} |A_{error}|dt\right], \tag{15}$$

where $A_{error} = \Delta F_i + \Delta P_{tie,i}$,
t_{sim} = simulation time,
N_{area} = number of interconnected areas,
ΔF_i = frequency deviation (FD) of i^{th} area,
$\Delta P_{tie,i}$ = deviation of tie line power i^{th} tie line power.

3 PIDD controller

Fast dynamic response and stability are the major advantages of PIDD controllers as compared to PI or PID controller [29]. Here, an effort has made to implement PIDD controller with a filter to diminish the detrimental outcomes of the high-frequency noises. Several integral controllers are already in use, including proportional-integral (PI), integral (I), integral-double derivative (IDD), and proportional-integral-derivative (PID) [34]. However, in microgrid systems, the PIDD controller is rarely used. An extra derivative controller is included with the derivative gain to configure the PIDD controller. The derivative unit improves the system steadiness by sinking the transient time and overshoot. Figure 5 shows the structure of a PIDD controller with block diagrams. PIDD controller in s-domain can be expressed as [35]:

$$PIDD_{TF} = K_P + \frac{K_I}{s} + K_{DD}s^2. \tag{16}$$

K_P, K_I and K_{DD} are the gain parameters of the PIDD controller.

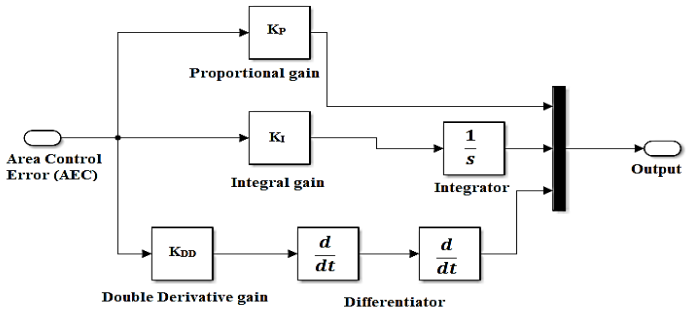

Figure 5. Structure of PIDD controller.

In an optimization problem, the parameters can be bounded as:

$$K_{Pi}^{min} \le K_{Pi} \le K_{Pi}^{max}, \tag{17}$$

$$K_{Ii}^{min} \le K_{Ii} \le K_{Ii}^{max}, \tag{18}$$

$$K_{DDi}^{min} \le K_{DDi} \le K_{DDi}^{max}, \tag{19}$$

where $\{K_{Pi}^{min}, K_{Ii}^{min}, K_{DDi}^{min}\}$ and $\{K_{Pi}^{max}, K_{Ii}^{max}, K_{DDi}^{max}\}$ are the minimum and maximum allowable limits of the gains of PIDD controllers.

4 hTLO-DE Technique

Teaching and learning-based optimization (TLO) [36] and differential evaluation (DE) [37] have been used in control applications to fine-tune controllers. Chen et al [38] also proposed a modified form of TLO. Local and self-learning approaches were used to improve the exploration capabilities. Together, the features of TLO and DE can provide an effective method for computing the global optimal values of the controller parameters. By integrating TLO with DE, a better exploration space can be created since TLO already has a learning approach. Consequently, a hTLO- DE is a useful tool for determining the global optimal values of controllers. The flowchart for the hTLO- DE approach [21] is shown in Figure 6.

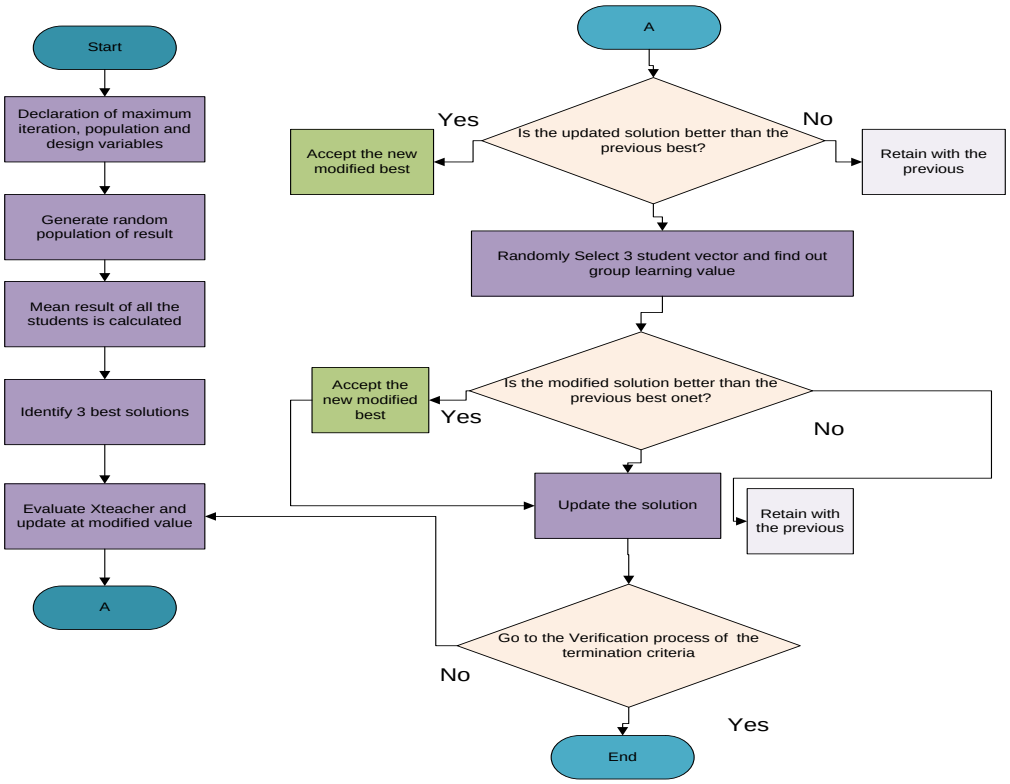

Figure 6. Flow-chart of hTLO-DE algorithm.

The TLO operation is conducted in two steps (i.e., teacher and student phases). During the teacher phase, the teacher is regarded the best answer, and each pupil (i.e., every other solution) attempts to improve in comparison to the teacher solution. However, this could cause the solution to become stuck by local minima. As a result, the DE mutation step is used to reach the instructor solution.

In TLO's instructor phase, the DE mutation procedure is carried out. Without seeing the best solution, a teacher solution $X_{teacher}$ is assessed by taking three best solutions (i.e., X^i, X^m, X^n) and using the mutation factor M as per (20). This aids to circumvent local minima and escort students out of local minima. The situation of each student (X_{mod}^i) is obtained by association with $X_{teacher}$ as per (21), where X_{mean} is the mean of all resolutions and T_f^i is the teacher factor of i^{th} iteration.

$$X_{teacher} = X^i + M(X^m - X^n) \tag{20}$$

$$X^i_{mod} = X^i + rand(0,1)\left[X_{teacher} - (T^i_f * X_{mean})\right] \tag{21}$$

In the student/learner phase, students work together to expand their knowledge. Here, each student has the opportunity to interact with another student (one-on-one learning) and expand their knowledge. Group learning can help improve the effectiveness of the process (i.e., many-to-one learning). In this case, using DE to apply mutation would ensure that each student learns from a group of students.

The mutation process is considered during the learning phase via the mutation factor *M* according to (22) and (23). The use of mutation during the learning phase improves and accelerates the improvement of student solutions, leading to faster convergence of the optimization problem. Compared to one-to-one learning, many-to-one learning (i.e., group learning) is more successful.

$$X_{Group} = X_j + M(X_k - X_l) \tag{22}$$

$$X^i_{mod,student} = X^i + rand(0,1)\left[X^i - X_{Group}\right] \tag{23}$$

Here, three students X_k , X_j , X_l are selected such as X^i not equals to X_k, X_j or X_l and, the group learning value X_{Group} is assessed as (22). Thereafter, the process of group learning is completed by each student X^i as per (23) to generate the value of new position $X^i_{mod.student}$. Thus, the optimal result is attained with lesser number of iterations and execution time. The population size (*K*) and maximum iteration (I_{max}) are retained at 50 and 100, respectively. A few unconstrained and constrained benchmark functions are used to validate the suggested optimization strategy. In addition, the suggested controller and optimization approach is applied to a multi-area-multi-source system with step and dynamic load variation ranging from ±20% in the DEG area.

5 Results and Analysis

The DEG-WTG-battery based microgrid model is simulated in Matlab/SIMULINK with step load perturbations (SLPs) in all generating units, as illustrated in Figure 1. Responses of different controllers such as PI, PID, and PIDD, are evaluated individually while frequency bias (B_i) is held constant at area frequency response characteristics. The hTLO-DE approach is used to optimise the controller parameters.

The optimization process is conducted by minimising the performance index according to (1). The optimum limits of different controllers under nominal loading condition are listed in Table 1 where K_P, K_I, K_D and K_{DD} are called the of the proportional, integral, derivative and double derivative controller gains.

The dynamic responses of the system are investigated using the optimum controller parameter values. The settling times of DEG frequency deviation (ΔF_1), WTG frequency deviation (ΔF_2), energy storage frequency deviation (ΔF_3), DEG-WTG tie line power deviation ($\Delta Ptie_1$), WTG-battery tie line power deviation ($\Delta Ptie_2$), and DEG-battery tie line power deviation ($\Delta Ptie_3$), are shown in Figure 7(a)–(f), respectively. When compared with PI/PID controller, PIDD controllers show significantly shorter settling period. Furthermore, it is obvious that PIDD controllers produce fewer oscillations in frequencies and tie-line powers. Figure 8 displays the convergence characteristics of the hTLO-DE approach. It can clearly be seen that the proposed hTLO-DE algorithm gives the optimal results with fewer iterations.

Table 1. Gains of controllers for optimal values at nominal loading.

Controller	Gains	Optimum values		
		DEG	WTG	Battery
	K_P	1	1.3	8.4
	K_I	0.1	0.8	0.01
PIDD	K_{DD}	0.01	0.05	0.009
	K_P	1.2	1.5	6.7
PI	K_I	0.6	0.5	0.013

PID	K_P	0.9	1.2	6.3
	K_I	0.5	0.05	0.02
	K_D	0.02	0.01	0.009

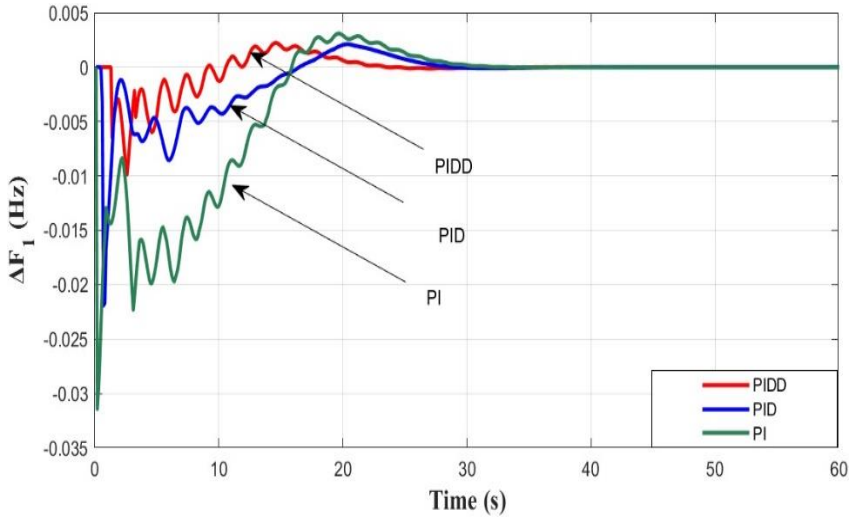

(a)

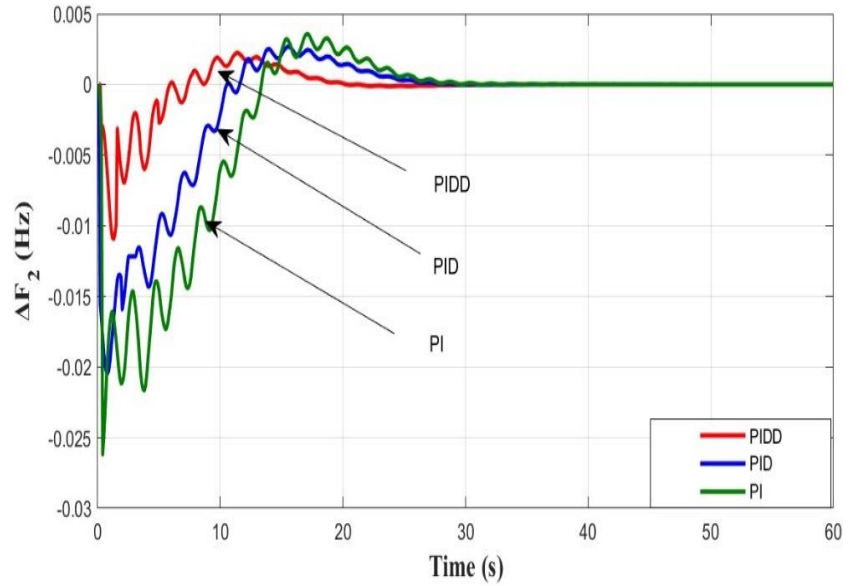

(b)

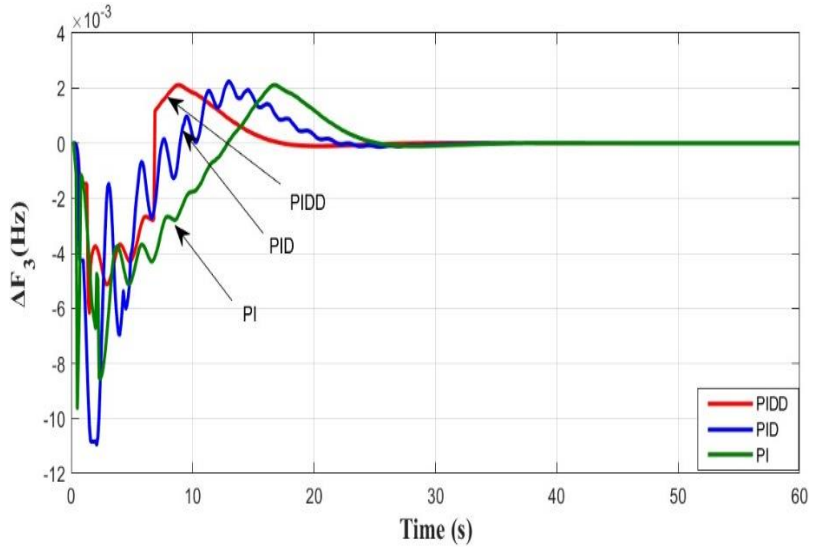
×10^-3
ΔF3 (Hz)
PIDD
PID
PI
Time (s)

(c)

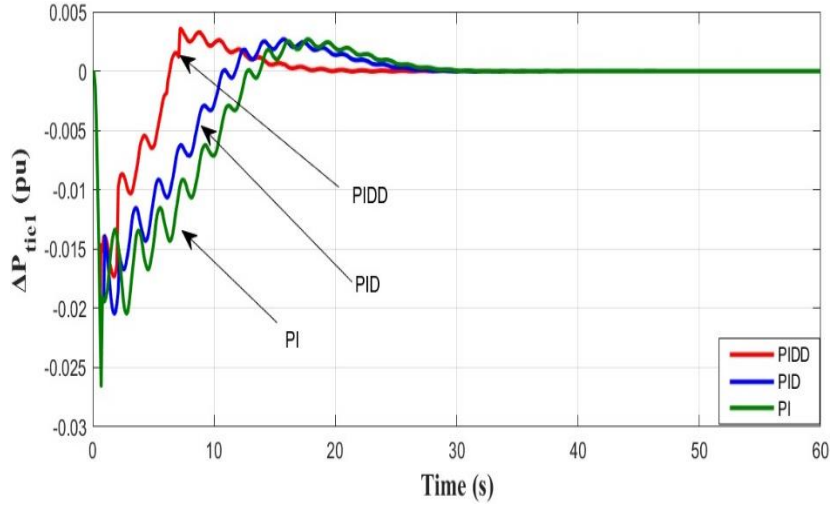
ΔPtie1 (pu)
PIDD
PID
PI
Time (s)

(d)

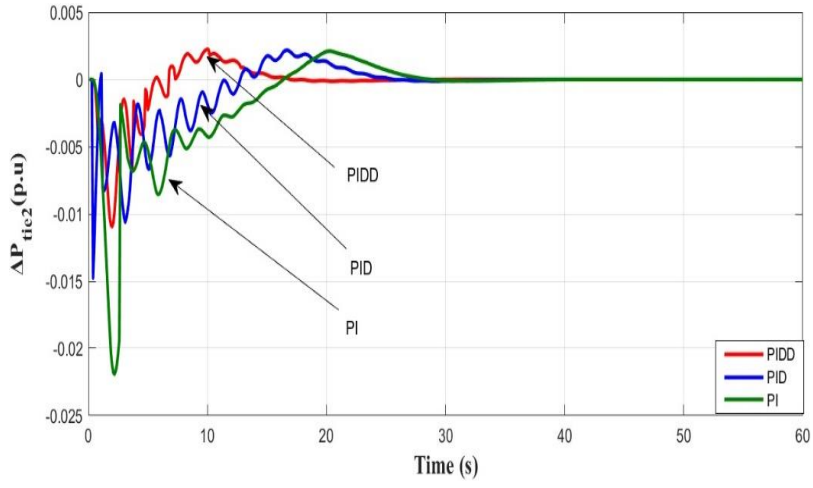
ΔPtie2 (p.u)
PIDD
PID
PI
Time (s)

(e)

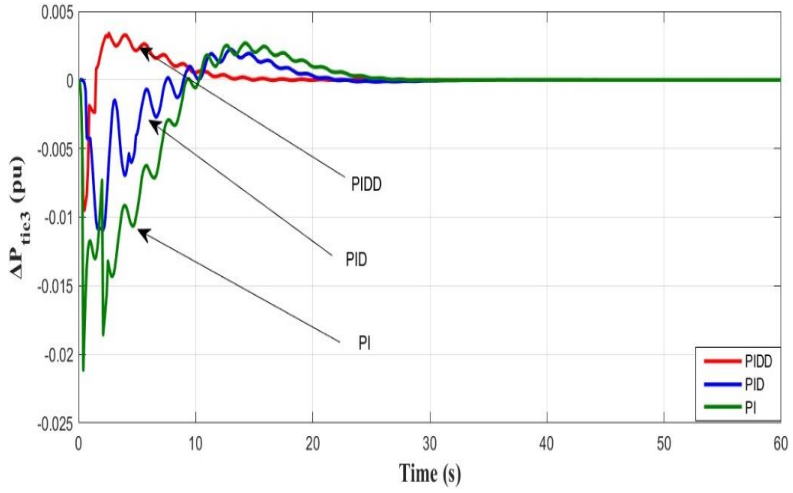

(f)

Figure 7. Time responses of (a) ΔF_1, (b) ΔF_2, (c) ΔF_3 and tie-line power deviations (d)ΔP_{tie1}, (e) ΔP_{tie2}, (f) ΔP_{tie3} for nominal loading condition.

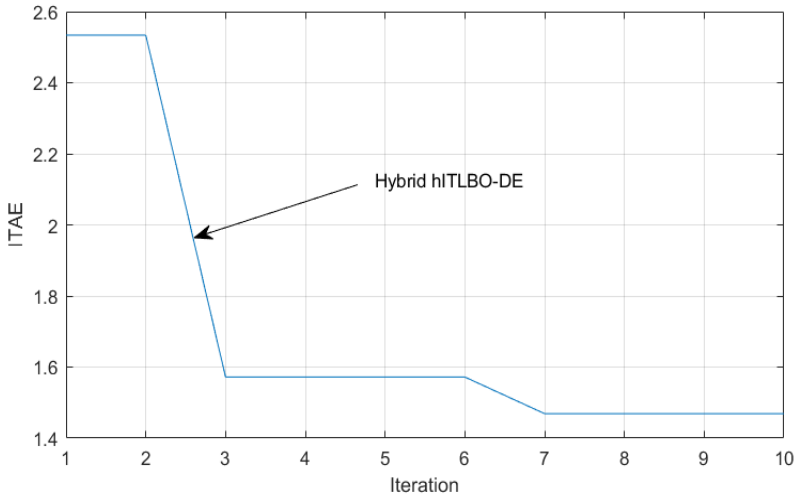

Figure 8. Convergence characteristics of hybrid hTLO-DE algorithm.

If a control scheme is not robust enough, the controller may not be able to cope with changes in system values.

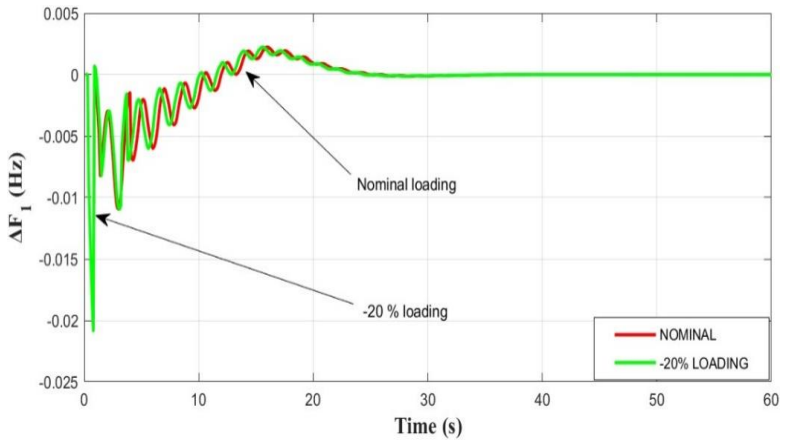

(a)

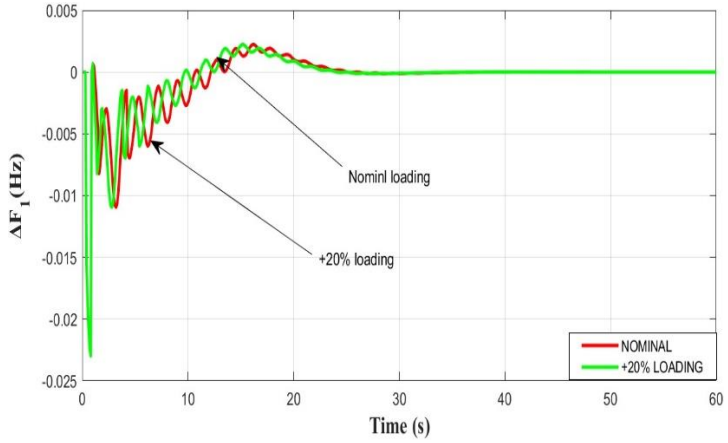

(b)

Figure 9. Sensitivity analysis with: (a) -20% nominal loading, and (b) +20% nominal loading in the DEG area.

Sensitivity analysis is performed to determine the robustness of the PIDD controller based LFC scheme. The computed controller parameters (i.e., K_P, K_I, K_{DD}) under nominal loading are considered constant for a large changes in system loading, i.e., ±20% nominal loading in the DEG area. In Figure 9 ((a)-(b)), the dynamic responses of area 1 frequency with normal loading and with ±20% nominal loading in the DEG area are shown. It is obvious from a critical examination of the dynamic responses in Figure 9 that, the parameters determined at nominal condition do not need to be reset to a wide range of system loading variations.

6 Conclusion

In this paper, a DEG-WTG-battery based microgrid system is modelled in terms of transfer functions to study LFC. In order to implement the LFC, PIDD controllers are adopted and an hTLO-DE technique is used to compute the controller gain parameters. System responses are investigated. The comparative analysis in terms of dynamic responses are performed against the commonly used PI/PID controllers. Furthermore, the robustness of the PIDD controller-based LFC scheme is tested with variable loadings. The results reveal that the suggested hTLO-DE tuned PIDD controllers are adequately reliable with faster dynamic responses for LFC in the renewable energy based microgrid application.

Appendix:

A. 1. The nominal parameters for the proposed system

$f = 50$ Hz, $T_{12} = T_{13} = T_{21} = T_{23} = T_{31} = T_{32} = 0.07$ s, $B_1 = B_2 = 0.425$, $R_1 = R_2 = 2.4$, $t_{g1} = t_{g2} = 0.2$ s, $t_{t1} = t_{t2} = 0.3$ s, $c_2 = 0.12$, $t_1 = t_{r2} = 20$ s, $k_{p1} = k_{p2} = 120$, $t_{p1} = t_{p2} = 20$ s, $T_{CON} = 0.0110$ s, $K_{EV} = 0.0012$, $T_{EV} = 0.09$ s, $N_{EV} = 0.1$.

References

[1] Dhillon, Sukhwinder Singh, Lather, J.S., Marwaha, S.: *Multi objective load frequency control using hybrid bacterial foraging and particle swarm optimized PI controller*, International Journal of Electrical Power & Energy Systems, 79 (2016), 196–209. doi:10.1016/j.ijepes.2016.01.012 .

[2] M. R. Khalghani, M. H. Khooban, E. Mahboubi-moghaddam, N. Vafamand, M. Goodarzi.: *A self-tuning load frequency control strategy for microgrids:* Human brain emotional learning. 75 (2016), 311-319. doi:10.1016/j.ijepes.2015.08.026 .

[3] Liu, Yan.:*Continuous dependence for a thermal convection model with temperature-dependent solubility*, Applied Mathematics and Computation, 308 (2017), 18–30. doi:10.1016/j.amc.2017.03.004.

[4] Gao, Wei, Darvishan, Ayda, Toghani, Mohammad, Mohammadi, Mohsen, Abedinia, Oveis, Ghadimi, Noradin.: *Different states of multi-block based forecast engine for price and load prediction,* International Journal of Electrical Power & Energy Systems, 104(2019), 423–435. doi:10.1016/j.ijepes.2018.07.014 .

[5] Kundur, P. : Power System Stability and Control(8th ed.), Tata McGraw-Hill, 2009.

[6] Guerrero, J.M., Vasquez, J.C., Matas, J., de Vicuna, L.G., Castilla, M.: *Hierarchical Control of Droop-Controlled AC and DC Microgrids,* A General Approach Toward Standardization, 58(2011)1, 158–172. doi:10.1109/tie.2010.2066534 .

[7] Bevrani, H, Daneshmand, P.R. : *Fuzzy Logic-Based Load-Frequency Control Concerning High Penetration of Wind Turbines* , IEEE systems journal, *6(2012)1 , 173–180.* doi:10.1109/jsyst.2011.2163028.

[8] Yesil, Engin.: *Interval type-2 fuzzy PID load frequency controller using Big Bang–Big Crunch optimization.* Applied Soft Computing, 15(2014), 100–112. doi:10.1016/j.asoc.2013.10.031 .

[9] Zheng, Shiqi; Tang, Xiaoqi; Song, Bao; Lu, Shaowu; Ye, Bosheng (2013). *Stable adaptive PI control for permanent magnet synchronous motor drive based on improved JITL technique. ISA Transactions, 52(4), 539–549.* doi:10.1016/j.isatra.2013.03.002 .

[10] Yang, Jun, Zeng, Zhili, Tang, Yufei, Yan, Jun, He, Haibo, Wu, Yunliang .: *Load Frequency Control in Isolated Micro-Grids with Electrical Vehicles Based on Multivariable Generalized Predictive Theory*. Energies, 8 (2015)3, 2145–2164. doi:10.3390/en8032145.

[11] Khooban, Mohammad-Hassan, Niknam, Taher; Blaabjerg, Frede, Davari, Pooya; Dragicevic, Tomislav .: *A robust adaptive load frequency control for micro-grids,* ISA Transactions,(2016) doi:10.1016/j.isatra.2016.07.002 .

[12] Gao, W., Yan, L., Saeedi, M.H., Saberi Nik, H. : *Ultimate bound estimation set and chaos synchronization for a financial risk system,* Mathematics and Computers in Simulation, (2018), doi:10.1016/j.matcom.2018.06.006 .

[13] Nejad, Hadi Chahkandi, Farshad, Mohsen, Rahatabad, Fereidoun Nowshiravan, Khayat, Omid.: *Gradient-based back-propagation dynamical iterative learning scheme for the neuro-fuzzy inference system,* Expert Systems, 33(2016)1, 70–76. doi:10.1111/exsy.12131 .

[14] Rastegar, Saeed, Babaeian, Amir; Bandarabadi, Mojtaba, Toopchi, Yashar : *Airplane detection and tracking using wavelet features and SVM classifier,* 41st Southeastern Symposium on System Theory, (2009), 64–67. doi:10.1109/SSST.2009. 4806823 .

[15] Mohammadi, Mohsen, Talebpour, Faraz, Safaee, Esmaeil; Ghadimi, Noradin, Abedinia, Oveis.: *Small-Scale Building Load Forecast based on Hybrid Forecast Engine,* Neural Processing Letters, (2017)doi:10.1007/s11063-017-9723-2.

[16] Debbarma, Sanjoy, Saikia, Lalit Chandra; Sinha, Nidul.: *Automatic generation control using two degree of freedom fractional order PID controller*, International Journal of Electrical Power & Energy Systems, 58 (2014), 120–129. doi:10.1016/j.ijepes.2014.01.011 .

[17] Ali, E., Elazim ,Abd, S :Bfoa based design of pid controller for two area load frequency control with nonlinearities, Int. Journal of Electrical Power & Energy Systems,. 51 (2013), 224–231.

[18] Mohanty, Banaja, Hota, Prakash Kumar .: *Comparative performance analysis of fruit fly optimisation algorithm for multi-area multi-source automatic generation control under deregulated environment*, IET Generation, Transmission & Distribution, 9 (2015)14, 1845–1855. doi:10.1049/iet-gtd.2015.0284 .

[19] Dash, Puja, Saikia, Lalit Chandra, Sinha, Nidul.: *Comparison of performances of several Cuckoo search algorithm based 2DOF controllers in AGC of multi-area thermal system*, International Journal of Electrical Power & Energy Systems, 55(2014), 429–436. doi:10.1016/j.ijepes.2013.09.034 .

[20] Shankar, Ravi, Pradhan, S.R., Chatterjee, Kalyan; Mandal, Rajasi .: *A comprehensive state of the art literature survey on LFC mechanism for power system*, Renewable and Sustainable Energy Reviews, 76 (2017), 1185–1207. doi:10.1016/J.RSER.2017.02.064 .

[21] Behera, Aurobindo; Panigrahi, Tapas Kumar; Ray, Prakash K.; Sahoo, Arun Kumar .: A novel cascaded PID controller for automatic generation control analysis with renewable sources, IEEE/CAA Journal of Automatica Sinica, (2019), 1–14. doi:10.1109/JAS.2019.1911666 .

[22] Panwar, Akhilesh; Sharma, Gulshan, Nasiruddin, Ibraheem, Bansal, R.C.: *Frequency stabilization of hydro–hydro power system using hybrid bacteria foraging PSO with UPFC and HAE*, Electric Power Systems Research, 161 (2018), 74–85. doi:10.1016/j.epsr.2018.03.027 .

[23] Saikia ,L. C., Nanda , J., Mishra , S : Performance comparison of several classical controllers in agc for multi-area interconnected thermal system, Int. Journal of Electrical Power & Energy Systems,. 33 (2011), 394–401.

[24] Sahu,R. K, Pamda, S, Padhan, S : A hybrid firefly algorithm and pattern search technique for automatic generation control of multi area power systems, Int. Journal of Electrical Power & Energy Systems, 64 (2015), 9–23

[25] Parmar,K. S, Majhi, S, Kothari, D, : Load frequency control of a realistic power system with multi-source power generation, Int. Journal of Electrical Power & Energy Systems, 42 (2012), 426–433.

[26] Sahu, B. K, Pati, S, Mohanti, P. K, Panda, S : Teaching-Learning based optimization algorithm based fuzzy-pid controller for automatic generation control of multi-area power system, Applied Soft Computing, 27 (2015), 240–249,

[27] Sahu, Rabindra Kumar, Gorripotu, Tulasichandra Sekhar; Panda, Sidhartha .: *Automatic generation control of multi-area power systems with diverse energy sources using Teaching Learning Based Optimization algorithm.* Engineering Science and Technology, an International Journal,*(2015)* doi:10.1016/j.jestch.2015.07.011 .

[28] Dash, P, Saikia, L. C, Sinha, N : Automatic generation control of multi area thermal system using bat algorithm optimized PD-PID cascade controller, Int. Journal of Electrical Power & Energy Systems, 68 (2015), 364–372.

[29] Dash, P, Saikia, L. C, Sinha, N : Flower pollination algorithm optimized PI-PD cascade controller in automatic generation control of a multi-area power system, Int. Journal of Electrical Power & Energy Systems, 82 (2016), 19–28

[30] Panigrahi. T, Dash, P, Hota, P : A self-tuning optimised unscented kalman filter for voltage flicker and harmonic estimation, Int. J. of Power and Energy Conversion, 2 (2010) , 250–278

[31] Barisal , A., Panigrahi , T., Mishra, S. : A hybrid pso-levy flight algorithm based fuzzy pid controller for automatic generation control of multi area power systems: fuzzy based hybrid pso for automatic generation control, Int. J. of Power and Energy Conversion,. 6 (2017) , 42–63

[32] Fathy, Ahmed; Kassem, Ahmed M.: *Antlion optimizer-ANFIS load frequency control for multi-interconnected plants comprising photovoltaic and wind turbine*, ISA Transactions, (2018), doi:10.1016/j.isatra.2018.11.035 .

[33] Izadkhast, Seyedmahdi, Garcia-Gonzalez, Pablo, Frias, Pablo; Bauer, Pavol.: *Design of Plug-in Electric Vehicle's Frequency-Droop Controller for Primary Frequency Control and Performance Assessment*, IEEE Transactions on Power Systems, (2017), 4241 - 4254. doi:10.1109/TPWRS.2017.2661241 .

[34] Nanda, J, and Saikia, L.C.: Comparison of performances of several types of classical controller in automatic generation control for an interconnected multi-area thermal system. *2008 Australasian Universities Power Engineering Conference*, Sydney, NSW, (2008), 1-6.

[35] Navuri, P.K, Boddepalli. M.K.: *Performance Analysis of PIDD Controllers for Automatic Load Frequency Control of Multi-area Power System*, *IJCA*, 33 (2020) 3, 366-377 .

[36] Debbarma, Sanjoy, Dutta, Arunima .: *Utilizing Electric Vehicles for LFC in Restructured Power Systems Using Fractional Order Controller, IEEE Transactions on Smart Grid*, (2016), 2554 – 2564, doi:10.1109/tsg.2016.2527821 .

[37] Sahu, Rabindra Kumar, Gorripotu, Tulasichandra Sekhar; Panda, Sidhartha .: *Automatic generation control of multi-area power systems with diverse energy sources using Teaching Learning Based Optimization algorithm.* Engineering Science and Technology, an International Journal,*(2015)* doi:10.1016/j.jestch.2015.07.011 .

[38] Chen, Debao, Zou, Feng, Li, Zheng; Wang, Jiangtao, Li, Suwen.: *An improved teaching–learning-based optimization algorithm for solving global optimization problem*, Information Sciences, 297 (2015), 171–190. doi:10.1016/j.ins.2014.11.001 .